

This is the author's accepted manuscript of the following article:

Mohey-Elsaeed Omnia, Marei Waleed F. A., Fouladi-Nashta Ali A., El-Saba Abdel-Aleem A. (2015) Histochemical structure and immunolocalisation of the hyaluronan system in the dromedary oviduct. *Reproduction, Fertility and Development* 28, 936-947.

The final publication is available at <http://dx.doi.org/10.1071/RD14187>.

The full details of the published version of the article are as follows:

TITLE: Histochemical structure and immunolocalisation of the hyaluronan system in the dromedary oviduct

AUTHORS: Mohey-Elsaeed Omnia, Marei Waleed F. A., **Fouladi-Nashta Ali A.**, El-Saba Abdel-Aleem A.

JOURNAL TITLE: *Reproduction, Fertility and Development*

PUBLICATION DATE: 7 January 2015 (online)

PUBLISHER: CSIRO Publishing

DOI: 10.1071/RD14187

Regulation and roles of the hyaluronan system in mammalian reproduction

Omnia Mohey-Elsaeed ^A, Waleed F. A. Marei ^{B,D}, Ali A. Fouladi-Nashta ^C and Abdel-Aleem A. El-Saba ^A

^A Department of Cytology and Histology, Faculty of Veterinary Medicine, Cairo University, Giza 12211, Egypt.

^B Department of Theriogenology, Faculty of Veterinary Medicine, Cairo University, Giza 12211, Egypt.

^C Department of Comparative Biomedical Sciences, Royal Veterinary College, Hatfield AL9 7TA, UK.

^D Corresponding author. Email: wmarei@staff.cu.edu.eg

1 Abstract

2 We investigated the local modulation of some histochemical properties of oviducts of the
3 dromedary (*Camelus dromedarius*), focusing on the immunolocalisation of hyaluronic acid (HA)
4 synthases (HAS2 and HAS3), hyaluronidases (HYAL2 and HYAL1) and the HA receptor CD44 in the
5 ampulla and isthmus. Abundant acidic mucopolysaccharides (glycosaminoglycans) were detected by
6 Alcian blue staining along the luminal surface of both ciliated and non-ciliated epithelial cells (LE).
7 Staining for HAS2 was higher in the primary epithelial folds of the ampulla compared with the
8 isthmus, especially in secretory cells, adluminal epithelial surface and supranuclear cell domain.
9 HAS3 staining was stronger in the LE of the isthmus than ampulla. HYAL2 was detected in the LE in
10 the ampulla and isthmus and was more intense in the adluminal projections of secretory cells. HYAL1
11 was weakly detected in the LE with no difference between the ampulla and isthmus. Strong CD44
12 immunostaining was present in the LE of the ampulla and isthmus. CD44 staining was higher in
13 secretory cells than in ciliated epithelial cells and was higher in the supranuclear region than the
14 basal region of the cytoplasm. In conclusion, we provide evidence that HA synthesis and turnover
15 occur in the camel oviduct. Differences in HAS2 and HAS3 expression suggest regional differences in
16 the molecular size of HA secreted in oviductal fluid that may influence oviduct–gamete interaction in
17 the camel.

18

19 **Introduction**

20 The oviduct is a highly specialised ‘reproductive organ’ (Menezo and Guerin 1997) in which many
21 reproductive events take place, such as sperm transport and capacitation, oocyte transport and
22 fertilisation, and early embryo development and transport to the uterus. Most of these events are
23 regulated by the secretory function of oviductal lining epithelium that contributes to oviductal
24 secretion with various materials that provide a suitable microenvironment for these events to occur.
25 Some of the functions of the oviduct are also regulated by direct interaction between gametes and
26 oviductal epithelial cells. The oviduct is divided into three regions: the infundibulum, ampulla and
27 isthmus. After sperm transport and capacitation in the isthmus and ovum pick up by the infundibulum,
28 fertilisation occurs in the ampulla (Hawk 1987). These regional roles require and suggest specific
29 regional micromorphology and function, and adjustments in the biochemical composition of the
30 oviductal fluid. Differences in protein and glycoprotein composition of oviductal secretions between
31 the ampulla and isthmus were observed many years ago (Nieder and Macon 1987; Buhi et al. 1990).
32 Explanted sections of ampulla of the oviduct, but not explants from the isthmus or uterus, were able
33 to support mouse embryonic development (Whittingham 1968). These findings suggest that gradient
34 changes in the oviductal microenvironment are required to facilitate specific roles for each region.
35 Knowledge of these differences should provide scientific bases for the development of assisted
36 reproductive technologies; however, to date, little is known in this regard.

37 Oviductal fluid contains a vast number of components that may influence oviduct–gamete interactions
38 and support early embryo development. Avilés et al. (2010) listed more than 160 different
39 components of the oviductal fluid that are required for optimal development of the different
40 processes that take place in the oviduct. Among those factors, oviductal glycans are of special interest.
41 Glycosaminoglycans have received little research attention despite evidence of their critical role
42 during oocyte maturation (Teixeira Gomes et al. 2009; Marei et al. 2012; Raheem et al. 2013) and
43 embryo development (Marei et al. 2013).

44 Hyaluronic acid (HA), a non-sulfated glycosaminoglycan, is a major constituent of the extracellular
45 matrix (ECM) abundant in most tissues and is also present in body fluids. HA can be found in oviductal
46 (Tienthai et al. 2000) and uterine (Teixeira Gomes et al. 2009; Raheem et al. 2013) fluids. There is
47 increasing evidence that HA is not only present as a space filler, but is also involved in various biological
48 functions that involve binding to specific receptors and initiation of cell signalling. It is also evident
49 that the function of HA is highly dependent on its molecular weight (Toole 2004). HA is a linear polymer
50 composed of repeating disaccharides of glucouronic acid and N-acetyl glucosamine synthesised by the
51 HA synthases HAS1, HAS2 and HAS3 (Spicer et al. 1997). These synthases are located at the inner

52 surface of the plasma membrane (Prehm 1984) and extrude the growing polymer chain through the
53 membrane into the pericellular space (Weigel et al. 1997). Each HAS is characterised by a different
54 molecular stability and average length (molecular size) of the HA produced (Dougherty and van de Rijn
55 1993; Crater and van de Rijn 1995; Itano and Kimata 2002; Stern 2005).

56 HA has an extraordinary high turnover rate. HA is degraded by a family of enzymes named
57 hyaluronidases (HYALs). HYAL1 and HYAL2 are the most common HYALs in somatic cells (Csoka et al.
58 2001). HYAL2 breaks down high molecular weight HA into 20–30 kDa fragments but has no effect on
59 low molecular weight HA fragments (Lepperdinger et al. 1998).

60 The major cell surface receptor for HA is a membrane glycoprotein called CD44, which has high binding
61 affinity for HA (Aruffo et al. 1990). The ability of a single molecule of HA to bind to multiple CD44
62 receptor sites (Underhill 1992) enables the involvement of this receptor in cell–cell and cell–ECM
63 interactions, adhesion and migration (Lesley et al. 1993). CD44–HA interactions also mediate
64 endocytosis of exogenous HA, leading to its degradation by lysosomal HYAL1 (McCourt 1999). CD44–
65 HA interactions are also known to initiate cell signalling, which induces cytokine secretion, stimulates
66 expression of growth factor receptors, protects against apoptosis and enhances cell proliferation and
67 cell motility (Stern et al. 2006).

68 The dromedary, also known as the Arabian camel, is an important livestock in many countries,
69 including Egypt, in addition to its economic importance in tourism and camel races in some countries.
70 Assisted reproduction in camels is still challenging compared with cattle because camels are
71 characterised by late puberty, seasonal breeding and induced ovulation (Ismail 1987; Skidmore 2003).
72 Most IVF, capacitation, fertilisation and embryo transfer procedures are extrapolated from cattle and
73 can be optimised for camel oocytes and semen. Studying the histochemical characteristics and HA
74 system in the camel oviduct could provide some basic knowledge required for the development of
75 assisted reproductive technologies in this species. This may also have some application in other
76 species.

77 The present study was performed to investigate the local modulation of some histochemical
78 properties in the ampulla and isthmus regions of the oviduct during the breeding season of the camel,
79 focusing on immunohistochemical changes of HA system (HAS, HYALs and CD44).

80 **Materials and methods**

81 *Sample Collection*

82 Reproductive tracts of adult female camels (*Camelus dromedarius*; n = 5) were collected from a local
83 abattoir during the breeding season. Tracts with ovaries containing a large anovulatory follicle (1–1.9
84 cm in diameter) were selected. Ipsilateral oviducts were immediately dissected from the surrounding
85 connective tissue and from the uterus. Sections from the ampulla (1–3 cm from the infundibulum) and
86 isthmus (1–2 cm from the uterotubal junction) were immediately fixed in 10% buffered formalin for 48
87 h. Tissues were then rinsed and kept in 70% ethanol until processing and embedding in paraffin blocks.

88 *Histological and histochemical examination*

89 Tissue blocks were cut into 5- μ m sections, mounted on glass slides and left to dry. Sections were
90 rehydrated through a series of decreasing concentrations of ethanol. General histological structure was
91 examined by haematoxylin and eosin (H&E) staining or Crossman trichrome staining following
92 conventional protocols (Bancroft and Stevens 1982). Some sections were stained using the periodic
93 acid-Schiff (PAS) reaction to examine neutral mucopolysaccharides or with Alcian blue (pH 2.5) to
94 locate acidic mucopolysaccharides (Bancroft and Stevens 1982).

95 *Localisation of the HA system by immunohistochemistry*

96 Protein expression of HAS2, HAS3, HYAL1, HYAL2 and the HA receptor CD44 was determined by
97 immunohistochemistry (IHC) as described previously (Raheem et al. 2013), with some modifications.
98 Briefly, paraffin-embedded oviductal sections (5 μ m) mounted on superfrost slides were used. Antigen
99 retrieval was performed for 30 min in boiling sodium citrate (2.947 g L⁻¹, pH 6.0). Non-specific
100 binding was blocked using 10% (v/v) normal horse serum (Dako, Glostrup, Denmark) and 4% (w/v)
101 bovine serum albumin (BSA) in phosphate-buffered saline (PBS) for 45 min. Endogenous peroxidase
102 was blocked using hydrogen peroxide 3% v/v in methanol for 30 min. Primary antibodies used for
103 immunostaining were polyclonal rabbit anti-HAS2 (1 : 100; Sc-66916; Santa Cruz Biotechnology,
104 Santa Cruz, CA, USA), polyclonal rabbit anti-HAS3 (1 : 100; Sc-66917; Santa Cruz Biotechnology),
105 HYAL1 (1 : 200; HPA002112; Sigma, St Louis, MO, USA); HYAL2 (1 : 100; AB90004; Abcam,
106 Cambridge, UK) and monoclonal mouse anti-CD44v6 (1 : 200; MCA1730; AbD Serotec, Kidlington,
107 UK). Simultaneously, sections for negative controls were treated in the same way but replacing primary
108 antibody with normal rabbit or normal mouse IgGs (Santa Cruz Biotechnology) at the same
109 concentrations. The reaction was completed with horseradish peroxidase-conjugated polyclonal swine
110 anti-rabbit secondary antibody (1 : 200; P0217; Dako) or rabbit anti-mouse (1 : 200; P0260; Dako) and
111 visualised using diaminobenzidine (DAB; Vector Laboratories, Peterborough, UK). Nuclei were
112 counterstained with haematoxylin and differentiated using acid alcohol. Slides were examined under a
113 light microscope (DM500; Leica, Wetzlar, Germany) and images were captured using an attached
114 digital camera (ICC50 HD; Leica).

115 *Semiquantitative analysis of immunostaining*

116 Immunostaining was assessed semiquantitatively using histochemical score (HSCORE) as described
117 previously (Ponglowhapan et al. 2008). Briefly, the HSCORE was calculated by multiplying the
118 intensity (as a score of 0–3) of the brown DAB stain in a particular layer within the oviduct and the
119 percentage of that area stained (0–100%). The estimate was based on five random fields per section
120 from five different oviducts. Images were scored by two independent experienced assessors blinded to
121 the corresponding region.

122 *Statistical analysis*

123 Numerical data generated by HSCORE are summarised as the mean \pm s.e.m. T-tests were used to
124 compare HSCOREs of the ampulla and isthmus using SPSS version 21 (IBM SPSS Statistics for
125 Windows, Version 21.0. Armonk, NY: IBM Corp.). Two-tailed T-test at $P < 0.05$ was considered
126 significant.

127

128 **Results**

129 *Histology of the camel oviduct*

130 The wall of the camel oviduct appeared to consist of mucosa, submucosa, muscularis and outermost
131 serosa layers (Fig. 1). The mucosa of the ampulla consisted of large and numerous primary folds that
132 branched, forming secondary folds and sometimes tertiary folds (Fig. 1a). The epithelium was mainly
133 simple columnar ciliated and non-ciliated (secretory or peg) cells (Fig. 1b). The ciliated cells
134 contained oval or ovoid basally situated basophilic nuclei containing fine chromatin granules. Some
135 of the columnar ciliated cells were vacuolated. Peg cells were narrower than ciliated cells and
136 characterised by dome-shaped cytoplasmic projections protruding from the apical (luminal) surface
137 (Fig. 1b–d). The nuclei of peg cells were basal, elongated and flattened laterally, containing dense
138 chromatin granules. Morphological signs of secretory activity were evident in peg cells that possessed
139 more deeply stained cytoplasm by H&E and a vesicular and basally situated nucleus (Fig. 1b). Peg
140 cells were also strongly positive to PAS stain, indicating the presence of abundant neutral
141 polysaccharides (Fig. 1c), and also contained fine alcianophilic granules, especially in the
142 supranuclear region and the apical cytoplasmic projection as seen by Alcian blue staining (Fig. 1d),
143 indicating the presence of acidic polysaccharides.

144 The epithelium was separated from the lamina propria submucosa with a PAS-positive basement
145 membrane (Fig. 1c). The lamina propria submucosa was formed of a thin layer under the epithelium
146 and extended into the mucosal folds (Fig. 1e). It consisted of loose connective tissue (CT) and
147 sometimes contained a few leucocytes and small blood vessels. The CT of the lamina propria was
148 denser in the primary and secondary folds and less dense in the tertiary folds (Fig. 1a, f).

149 The tunica muscularis of the ampulla consisted mainly of inner circular and thin outer longitudinally
150 arranged smooth muscle fibres (Fig. 1e) that were positive to PAS (Fig. 1g).

151 The serosa consisted of loose CT with many blood vessels and some dispersed circular and
152 longitudinal bundles of smooth muscle fibres. The serosa was covered externally with simple
153 squamous mesothelium (Fig. 1h, i). The dispersed muscle bundles and the tunica intima of the
154 arterioles in the lamina propria and serosa were positive to PAS (Fig. 1g).

155 In the isthmus, the lumen was narrower than that of the ampulla with fewer primary folds and very
156 few secondary folds (Fig. 2a). The epithelium appeared to be high columnar to pseudostratified
157 columnar epithelium containing ciliated and non-ciliated cells as well as basal cells. (Fig. 2b–e). The
158 non-ciliated peg cells were less abundant and protruded less into the lumen compared with in the
159 ampulla. The reaction of these cells towards Alcian blue stain was restricted to the apical surface (Fig.
160 2d). Peg cells were also positive to PAS staining (Fig. 2e). The basal cells appeared triangular, faintly
161 stained with rounded nuclei (Fig. 2b).

162 The lamina propria was similar to that of the ampulla, whereas the tunica muscularis was very thick,
163 consisting of several alternating layers of circular and longitudinal smooth muscles (Fig. 2f–h). The
164 isthmus was covered by serosa composed of highly vascularised loose CT and mesothelium (Fig. 2a).

165 *Immunolocalisation of HAS2*

166 HAS2 immunostaining in the ampulla and isthmus was detected in the lamina epithelialis (LE),
167 muscularis, blood vessels and mesothelium of the serosa, whereas the lamina propria and CT of the
168 serosa were negative (Fig. 3a–g). In the LE of the ampulla, the intensity of HAS2 immunostaining was
169 moderate in the peripheral (primary) folds (Fig. 3a–c). Staining was stronger in the adluminal
170 epithelial surface and the supranuclear cell domain than in the basal cell compartment, and some
171 nuclei were strongly stained (Fig. 3b). Expression of HAS2 in secondary and tertiary folds of the LE in
172 the ampulla (Fig. 3c) and isthmus (Fig. 3e, f) was less than in primary folds of the ampulla (Fig. 3i).
173 Some nuclei were weakly stained. Expression of HAS2 in peg cells was relatively higher than in
174 ciliated epithelial cells, particularly in the dome-shaped part in the lumen in the ampulla. It was
175 noted that HAS2 staining was also strong at the mesothelium covering the serosa (Fig. 3f, g).
176 Negative controls revealed no immunostaining or background (Fig. 3h).

177 *Immunolocalisation of HAS3*

178 HAS3 immunostaining in ciliated and secretory cells of the LE of the isthmus was moderate and
179 relatively stronger compared with the LE of the ampulla, where HAS3 immunostaining was mainly
180 restricted to peg cells. The lamina propria was strongly stained in the ampulla, but not in the
181 isthmus. Moderate staining was also detected in the inner layer of the tunica muscularis in both the
182 ampulla and isthmus, whereas less intense staining in the outer layers was observed (Fig. 4a–d, g).
183 HAS3 staining was also detectable in the CT in the serosa (Fig. 4b, e). No immunostaining or
184 background was detected in negative controls (Fig. 4f).

185 *Immunolocalisation of HYAL2*

186 HYAL2 was detected in LE cells in the ampulla (Fig. 5a) and isthmus (Fig. 5b) and was more intense in
187 the adluminal projections of peg cells (Fig. 5c, d), which were more abundant in the ampulla. HYAL2
188 was weak in the lamina propria, moderate in the muscosa and serosa, and strong at the
189 mesothelium. No staining could be detected in the negative controls (Fig. 5e). There were no
190 significant differences in the localisation and intensity of HYAL2 staining between the ampulla and
191 isthmus (Fig. 5f).

192 *Immunolocalisation of HYAL1*

193 HYAL1 immunostaining was detected in the LE (Fig. 6) with no difference between the ampulla and
194 isthmus (Fig. 6a, b). Very weak HYAL1 staining was also observed in the lamina propria and
195 muscosa. A negative control is shown in Fig. 6c.

196 *Immunolocalisation of CD44*

197 Strong CD44 immunostaining was present in the LE of the ampulla and isthmus. CD44 staining was
198 higher in peg cells than ciliated epithelial cells and was higher in the supranuclear region than in the
199 basal region of the cytoplasm (Fig. 7a–d). CD44 immunostaining was high in the muscular layer as
200 well as in the smooth muscles of the blood vessels of the serosa and in the mesothelial lining of the
201 serosa (Fig. 7a, b). CD44 immunostaining was weak in the propria submucosa, but the fibrocytes
202 were strongly stained (Fig. 7d). This pattern of expression was similar to the pattern of PAS-positive
203 staining shown in the ampulla (Fig. 1c, g) and isthmus (Fig. 2e). A negative control is shown in Fig. 7e.
204 There were no significant differences in the HSCORE of CD44 staining intensity between the ampulla
205 and isthmus in different layers (Fig. 7f).

206 **Discussion**

207 The aim of the present study was to examine the histochemical properties of the camel oviduct,
208 focusing on the immunolocalisation of HAS, HYALs and the HA receptor CD44 in the ampulla and
209 isthmus regions. In the camel, the follicular cycle can be divided into a growth phase (~10 days), a
210 mature phase (~8 days) and a regression phase (~12 days; Skidmore et al. 1996). For the purpose of
211 the present study, oviducts ipsilateral to ovaries carrying dominant follicles ranging between 1 and
212 1.9 cm in diameter were selected. This follicular size has been shown previously to correspond with
213 the optimum time for mating because it is associated with the highest ovulation rates following
214 mating or buserelin injection (Skidmore et al. 1996).

215 The results of the present study show that the histological structure of the oviduct is similar to that
216 described before in the camel (Srikandakumar et al. 2011; Accogli et al. 2014) and other ruminants
217 (Abe 1996). Oviductal epithelium consists of a single layer of ciliated and non-ciliated columnar cells
218 (Srikandakumar et al. 2011). We observed that the epithelial cells were taller in the isthmus
219 compared with the ampulla and that non-ciliated peg cells were characterised by dome-shaped
220 projections on the luminal surface, particularly in the ampulla. These 'apical blebs' of peg cells have
221 been described in camel oviducts as a typical feature of the mature phase of the oestrous cycle
222 associated with the apocrine pattern of oviductal secretion (Accogli et al. 2014).

223

224 Plasma membranes of epithelial cells are organised into two distinct domains: the apical domain,
225 which faces the lumen, and the basolateral domain, which includes the rest of the cell (Wang and
226 Margolis 2007). These domains are separated by a ring of tight junctions, have different protein
227 compositions and are targets of different types of Golgi vesicles (Wang and Margolis 2007). These
228 differences may explain some of the differences in histochemical properties and immunolocalisation
229 of HA-related proteins in the LE of the ampulla and isthmus of the camel oviduct, as discussed
230 below.

231 We found that PAS and Alcian blue positive staining in the LE was restricted to the secretory cells,
232 particularly to the adluminal projections in both the ampulla and isthmus. This indicates the
233 presence of neutral and acidic polysaccharides in the oviductal secretions in the camel. This is in
234 accordance with a previous report in the camel (Accogli et al. 2014). Numerous glycoconjugates
235 were also reported in lama oviduct, some of which were shown to play a role in sperm binding to
236 oviductal epithelium (Apichela et al. 2010). Among the acidic polysaccharides that are positively
237 stained by Alcian blue, glycosaminoglycans, particularly HA, are of special interest because of their
238 role in fertilisation and embryo development. For this reason, we focused on the immunolocalisation
239 of the HA system in the ampulla and isthmus of the camel oviduct.

240 HAS2 is known to produce high molecular weight (HMW) HA ($>2 \times 10^3$ kDa), whereas HAS3 produces
241 $0.1\text{--}1 \times 10^3$ kDa HA (Stern et al. 2006). We examined HAS expression in camel oviducts using
242 immunohistochemistry to determine localisation within different layers of the oviduct at the ampulla
243 and isthmus. We found that HAS2 and HAS3 are expressed in the LE in both ciliated and secretory
244 cells. The expression of HAS2 in the LE was highest in the primary folds of the ampulla compared
245 with the isthmus, whereas HAS3 expression was higher in the isthmus than ampulla. This suggests
246 regional differences in the size of HA. There is growing evidence that HA plays a role in sperm
247 transport, capacitation, fertilisation and embryo development in many species, including cattle,
248 sheep and pigs (Tienthai et al. 2003a). Regional differences in the molecular size of HA in the
249 ampulla and isthmus may be required to regulate the role of HA in these events. The intensity of
250 immunostaining for both HAS2 and HAS3 was relatively higher in secretory cells compared with
251 ciliated cells, and higher in the adluminal epithelial surface and the supranuclear cell domain. This
252 indicates that HA is secreted from secretory cells as a constituent of oviductal fluid, and is also
253 produced by ciliated cells, perhaps to play a role in the interaction between the LE and gametes or
254 embryo. This observation is reinforced by abundant acidic mucopolysaccharides
255 (glycosaminoglycans) detected by Alcian blue staining along the apical (luminal) surface of both
256 ciliated and non-ciliated epithelial cells. In a previous report, the mRNA for HAS2 and HAS3 was

257 shown to be expressed in the bovine oviduct during the oestrous cycle (Ulbrich et al. 2004) and
258 although no significant differences could be detected between the ampulla and isthmus, the density
259 of electrophoresis bands from the HAS3 polymerase chain reaction (PCR) product was stronger in the
260 isthmus than ampulla. This was based on a whole-tissue homogenate and not representative of a
261 particular layer. In the same study, the relative intensity of the HA (detected using HA-binding
262 protein) appeared to be greater in the ampulla than in the isthmus (Ulbrich et al. 2004). This
263 suggests differences in the molecular weight of HA between the ampulla and isthmus in other
264 species.

265 We found differences in HAS2 and HAS3 expression in other layers of the oviduct. The CT of the
266 lamina propria extending in oviductal folds and surrounding the mucosa, as well as serosa, was
267 negative for HAS2 but strongly positive for HAS3. In human and porcine oviducts (Edelstam et al.
268 1991; Tienthai et al. 2000), bovine oviducts (Ulbrich et al. 2004) and bovine endometrium (Raheem
269 et al. 2013), hyaluronan has been localised to the entire lamina propria surrounding the LE and
270 extending into oviductal villi. The detection of HAS but not HA in the LE suggests that HA produced
271 by LE is directly secreted into oviductal fluid and thus lost during tissue processing for staining. We
272 found that HAS2 is weakly detected in the lamina propria and HAS3 is predominant, which suggests
273 that HA in the lamina propria is derived primarily from HAS3. It is also worth noting that we
274 observed positive HAS2 staining in some nuclei of the LE. HAS are localised at the plasma membrane;
275 thus, nuclear staining seems perplexing. In a previous study, HAS1 immunostaining was found in
276 nuclei of different layers of ovine endometrium (Raheem et al. 2013).

277 HA is a non-sulfated glycosaminoglycan. Another glycosaminoglycan, heparin, is found in oviductal
278 fluid (Bergqvist and Rodriguez-Martinez 2006) and was shown to be potent in maintaining sperm
279 motility and triggering capacitation in vitro in cattle (Parrish et al. 1994). It has been shown recently
280 that HA plays an important role during oocyte maturation (Marei et al. 2012) and preimplantation
281 embryo development (Marei et al. 2013). Of the different HA receptors, CD44 is a widely distributed
282 cell-surface receptor and is considered the main receptor for HA. In swine, exogenous HA improved
283 development of parthenogenetic embryo development in vitro (Toyokawa et al. 2005). This was
284 suggested to be mediated through a cellular response via CD44 because the effects of HA were
285 abolished in the presence of anti-CD44 antibodies (Toyokawa et al. 2005). In that study, the authors
286 also claimed that exogenous HA is accessible to its own receptor through the zona pellucida in order
287 to serve as a ligand. In the present study, we found that CD44 is expressed in LE cells in the ampulla
288 and isthmus. The intensity of CD44 staining was highest at the surface membrane and supranuclear
289 domain of mainly secretory cells. The apical cell surface localisation of CD44 corresponds to the cell

290 membrane HA receptor, and the supranuclear localisation may represent the internalised CD44. This
291 pattern of expression is very similar to that described previously in the lining epithelium of the
292 porcine oviduct (Tienthai et al. 2003b). In contrast, there was no evidence of epithelial staining of
293 CD44 in bovine oviducts using anti-porcine CD44 monoclonal antibody (Ulbrich et al. 2004). We
294 could not detect any significant difference in CD44 immunostaining between the ampulla and
295 isthmus. In contrast, in bovine oviduct, the mRNA expression of CD44 was found to be >10-fold
296 higher in the isthmus than ampulla (Ulbrich et al. 2004). However, because this expression is derived
297 from a whole-region transcript, the overall higher CD44 in the isthmus may be due to thicker muscle
298 layers that strongly express CD44.

299 The ligand-binding properties of CD44 are modulated by alternative splicing, creating CD44 variant
300 (CD44v) isoforms. The antibodies used to detect CD44 in the present study were specific for the
301 CD44v6 splice variant. On the basis of studies of tumour progression and metastatic potential, CD44
302 encoded by variant exon 6 (v6) is thought to be necessary for efficient HA adhesion (Menzel and Farr
303 1998). Thus, expression of this variant on the LE of camel oviducts suggests that CD44 can efficiently
304 bind HA and may mediate HA functions in the oviduct. Interactions between HA and CD44 and other
305 hyaladherins create a complex, hydrated microenvironment that supports and promotes the cellular
306 characteristics of proliferating and migrating cells (Toole 2004). CD44 also mediates a variety of
307 intracellular signalling cascades and interacts with cytoskeletal proteins that are essential for the
308 normal functioning of the cells.

309 HYAL1 and HYAL2 are the most abundant HYALs in somatic cells. HYAL2 is located on the cell surface
310 colocalised with CD44 and depolymerises HMW HA into fragment of 20–30 kDa in size. HYAL1 is a
311 lysosomal enzyme that degrades HA after internalisation by CD44 into tetra- and oligosaccharides
312 (Underhill 1992). It is important to note that we found HYAL2 to be expressed in a very similar
313 pattern to CD44 in the LE. HYAL2 is known to be colocalised with CD44 on the cell membrane.
314 Depolymerisation of extracellular HMW HA bound to CD44 into smaller fragments results in
315 disruption of HA–CD44 interactions, which initiates CD44 signalling (Ohno-Nakahara et al. 2004).
316 HYAL2 was also been shown to be expressed in bovine oviducts and the addition of HYAL2 to bovine
317 embryo culture in vitro enhanced embryo cell proliferation and resulted in better-quality embryos
318 (Marei et al. 2013). In addition, in the present study we detected weak immunostaining for HYAL1 in
319 the LE of the camel oviduct; HYAL1 is required for lysosomal degradation of HA after internalisation
320 by CD44. Intracellular HA fragments are biologically active and can bind to other receptors like
321 receptor for hyaluronan-mediated motility (RHAMM). These small-size HA fragments have been
322 associated with the induction of cytokine synthesis (Termeer et al. 2002; Shimada et al. 2008) and

323 upregulation of heat shock protein expression (Xu et al. 2002) and thus may influence embryo–
324 maternal interaction.

325 In conclusion, we provide evidence that enzymes required for HA synthesis and turnover are
326 expressed in the camel oviduct. Differences in HAS2 and HAS3 expression suggest regional
327 differences in HA molecular size. The HA receptor CD44 is also expressed in the LE of the ampulla
328 and isthmus. HA–CD44 interactions are suggested to be involved in oviduct–gamete interactions in
329 the camel.

330 **References**

- 331 Abe, H. (1996). The mammalian oviductal epithelium: regional variations in cytological and functional
332 aspects of the oviductal secretory cells. *Histol. Histopathol.* 11, 743–768.
- 333 Accogli, G., Monaco, D., El Bahrawy, K. A., El-Sayed, A. A., Ciannarella, F., Beneult, B., Lacalandra, G.
334 M., and Desantis, S. (2014). Morphological and glycan features of the camel oviduct epithelium. *Ann.*
335 *Anat.* 196, 197–205.
- 336 Apichela, S. A., Valz-Gianinet, J. N., Schuster, S., Jimenez-Diaz, M. A., Roldan-Olarte, E. M., and Miceli,
337 D. C. (2010). Lectin binding patterns and carbohydrate mediation of sperm binding to llama oviductal
338 cells in vitro. *Anim. Reprod. Sci.* 118, 344–353.
- 339 Aruffo, A., Stamenkovic, I., Melnick, M., Underhill, C. B., and Seed, B. (1990). CD44 is the principal cell
340 surface receptor for hyaluronate. *Cell* 61, 1303–1313.
- 341 Avilés, M., Gutiérrez-Adán, A., and Coy, P. (2010). Oviductal secretions: will they be key factors for the
342 future ARTs? *Mol. Hum. Reprod.* 16, 896–906.
- 343 Bancroft, J. D., and Stevens, A. (1982). 'Theory and practice of histological techniques.' 2nd edn.
344 (Churchill Livingstone: Edinburgh.)
- 345 Bergqvist, A. S., and Rodriguez-Martinez, H. (2006). Sulphated glycosaminoglycans (S-GAGs) and
346 syndecans in the bovine oviduct. *Anim. Reprod. Sci.* 93, 46–60.
- 347 Bui, W. C., Alvarez, I. M., Sudhipong, V., and Dones-Smith, M. M. (1990). Identification and
348 characterization of de novo-synthesized porcine oviductal secretory proteins. *Biol. Reprod.* 43, 929–
349 938.
- 350 Crater, D. L., and van de Rijn, I. (1995). Hyaluronic acid synthesis operon (HAS) expression in Group A
351 streptococci. *J. Biol. Chem.* 270, 18 452–18 458.
- 352 Csoka, A. B., Frost, G. I., and Stern, R. (2001). The six hyaluronidase-like genes in the human and mouse
353 genomes. *Matrix Biol.* 20, 499–508.
- 354 Dougherty, B. A., and van de Rijn, I. (1993). Molecular characterization of hasB from an operon
355 required for hyaluronic acid synthesis in Group A streptococci. Demonstration of UDP-glucose
356 dehydrogenase activity. *J. Biol. Chem.* 268, 7118–7124.

357 Edelstam, G. A., Lundkvist, O. E., Wells, A. F., and Laurent, T. C. (1991). Localization of hyaluronan in
358 regions of the human female reproductive tract. *J. Histochem. Cytochem.* 39, 1131–1135.

359 Hawk, H. W. (1987). Transport and fate of spermatozoa after insemination of cattle. *J. Dairy Sci.* 70,
360 1487–1503.

361 Ismail, S. T. (1987). A review of reproduction in the female camel (*Camelus dromedarius*).
362 *Theriogenology* 28, 363–371.

363 Itano, N., and Kimata, K. (2002). Mammalian hyaluronan synthases. *IUBMB Life* 54, 195–199.

364 Lepperdinger, G., Strobl, B., and Kreil, G. (1998). HYAL2, a human gene expressed in many cells,
365 encodes a lysosomal hyaluronidase with a novel type of specificity. *J. Biol. Chem.* 273, 22 466–22 470.

366 Lesley, J., Hyman, R., and Kincade, P. W. (1993). CD44 and its interaction with extracellular matrix.
367 *Adv. Immunol.* 54, 271–335.

368 Marei, W. F., Ghafari, F., and Fouladi-Nashta, A. A. (2012). Role of hyaluronic acid in maturation and
369 further early embryo development of bovine oocytes. *Theriogenology* 78, 670–677.

370 Marei, W. F., Salavati, M., and Fouladi-Nashta, A. A. (2013). Critical role of hyaluronidase-2 during
371 preimplantation embryo development. *Mol. Hum. Reprod.* 19, 590–599.

372 McCourt, P. A. (1999). How does the hyaluronan scrap-yard operate? *Matrix Biol.* 18, 427–432.

373 Menezes, Y., and Guerin, P. (1997). The mammalian oviduct: biochemistry and physiology. *Eur. J.*
374 *Obstet. Gynecol. Reprod. Biol.* 73, 99–104.

375 Menzel, E. J., and Farr, C. (1998). Hyaluronidase and its substrate hyaluronan: biochemistry, biological
376 activities and therapeutic uses. *Cancer Lett.* 131, 3–11.

377 Nieder, G. L., and Macon, G. R. (1987). Uterine and oviducal protein secretion during early pregnancy
378 in the mouse. *J. Reprod. Fertil.* 81, 287–294.

379 Ohno-Nakahara, M., Honda, K., Tanimoto, K., Tanaka, N., Doi, T., Suzuki, A., Yoneno, K., Nakatani, Y.,
380 Ueki, M., Ohno, S., Knudson, W., Knudson, C. B., and Tanne, K. (2004). Induction of CD44 and MMP
381 expression by hyaluronidase treatment of articular chondrocytes. *J. Biochem.* 135, 567–575.

382 Parrish, J. J., Susko-Parrish, J. L., Uguz, C., and First, N. L. (1994). Differences in the role of cyclic
383 adenosine 3',5'-monophosphate during capacitation of bovine sperm by heparin or oviduct fluid. *Biol.*
384 *Reprod.* 51, 1099–1108.

385 Ponglowhapan, S., Church, D. B., and Khalid, M. (2008). Differences in the expression of luteinizing
386 hormone and follicle-stimulating hormone receptors in the lower urinary tract between intact and
387 gonadectomised male and female dogs. *Domest. Anim. Endocrinol.* 34, 339–351.

388 Prehm, P. (1984). Hyaluronate is synthesized at plasma membranes. *Biochem. J.* 220, 597–600.

389 Raheem, K. A., Marei, W. F., Mifsud, K., Khalid, M., Wathes, D. C., and Fouladi-Nashta, A. A. (2013).
390 Regulation of the hyaluronan system in ovine endometrium by ovarian steroids. *Reproduction* 145,
391 491–504.

392 Shimada, M., Yanai, Y., Okazaki, T., Noma, N., Kawashima, I., Mori, T., and Richards, J. S. (2008).
393 Hyaluronan fragments generated by sperm-secreted hyaluronidase stimulate cytokine/chemokine
394 production via the TLR2 and TLR4 pathway in cumulus cells of ovulated COCs, which may enhance
395 fertilization. *Development* 135, 2001–2011.

396 Skidmore, J. A. (2003). The main challenges facing camel reproduction research in the 21st century.
397 *Reprod. Suppl.* 61, 37–47.

398 Skidmore, J. A., Billah, M., and Allen, W. R. (1996). The ovarian follicular wave pattern and induction
399 of ovulation in the mated and non-mated one-humped camel (*Camelus dromedarius*). *J. Reprod. Fertil.*
400 106, 185–192.

401 Spicer, A. P., Seldin, M. F., Olsen, A. S., Brown, N., Wells, D. E., Doggett, N. A., Itano, N., Kimata, K.,
402 Inazawa, J., and McDonald, J. A. (1997). Chromosomal localization of the human and mouse
403 hyaluronan synthase genes. *Genomics* 41, 493–497.

404 Srikandakumar, A., Johnson, E. H., Mahgoub, O., Kadim, I. T., and Al-Ajmi, D. S. (2011). Anatomy and
405 histology of the female reproductive tract of the arabian camel. *Emir. J. Agric. Sci.* 13, 23–26.

406 Stern, R. (2005). Hyaluronan metabolism: a major paradox in cancer biology. *Pathol. Biol. (Paris)* 53,
407 372–382.

408 Stern, R., Asari, A. A., and Sugahara, K. N. (2006). Hyaluronan fragments: an information-rich system.
409 *Eur. J. Cell Biol.* 85, 699–715.

410 Teixeira Gomes, R. C., Verna, C., Nader, H. B., dos Santos Simoes, R., Dreyfuss, J. L., Martins, J. R.,
411 Baracat, E. C., de Jesus Simoes, M., and Soares, J. M. (2009). Concentration and distribution of
412 hyaluronic acid in mouse uterus throughout the estrous cycle. *Fertil. Steril.* 92, 785–792.

413 Termeer, C., Benedix, F., Sleeman, J., Fieber, C., Voith, U., Ahrens, T., Miyake, K., Freudenberg, M.,
414 Galanos, C., and Simon, J. C. (2002). Oligosaccharides of hyaluronan activate dendritic cells via Toll-
415 like receptor 4. *J. Exp. Med.* 195, 99–111.

416 Tienthai, P., Kjellen, L., Pertoft, H., Suzuki, K., and Rodriguez-Martinez, H. (2000). Localization and
417 quantitation of hyaluronan and sulfated glycosaminoglycans in the tissues and intraluminal fluid of
418 the pig oviduct. *Reprod. Fertil. Dev.* 12, 173–182.

419 Tienthai, P., Kimura, N., Heldin, P., Sato, E., and Rodriguez-Martinez, H. (2003a). Expression of
420 hyaluronan synthase-3 in porcine oviducal epithelium during oestrus. *Reprod. Fertil. Dev.* 15, 99–105.

421 Tienthai, P., Yokoo, M., Kimura, N., Heldin, P., Sato, E., and Rodriguez-Martinez, H. (2003b).
422 Immunohistochemical localization and expression of the hyaluronan receptor CD44 in the epithelium
423 of the pig oviduct during oestrus. *Reproduction* 125, 119–132.

424 Toole, B. P. (2004). Hyaluronan: from extracellular glue to pericellular cue. *Nat. Rev. Cancer* 4, 528–
425 539.

426 Toyokawa, K., Harayama, H., and Miyake, M. (2005). Exogenous hyaluronic acid enhances porcine
427 parthenogenetic embryo development in vitro possibly mediated by CD44. *Theriogenology* 64, 378–
428 392.

429 Ulbrich, S. E., Schoenfelder, M., Thoene, S., and Einspanier, R. (2004). Hyaluronan in the bovine
430 oviduct: modulation of synthases and receptors during the estrous cycle. *Mol. Cell. Endocrinol.* 214,
431 9–18.

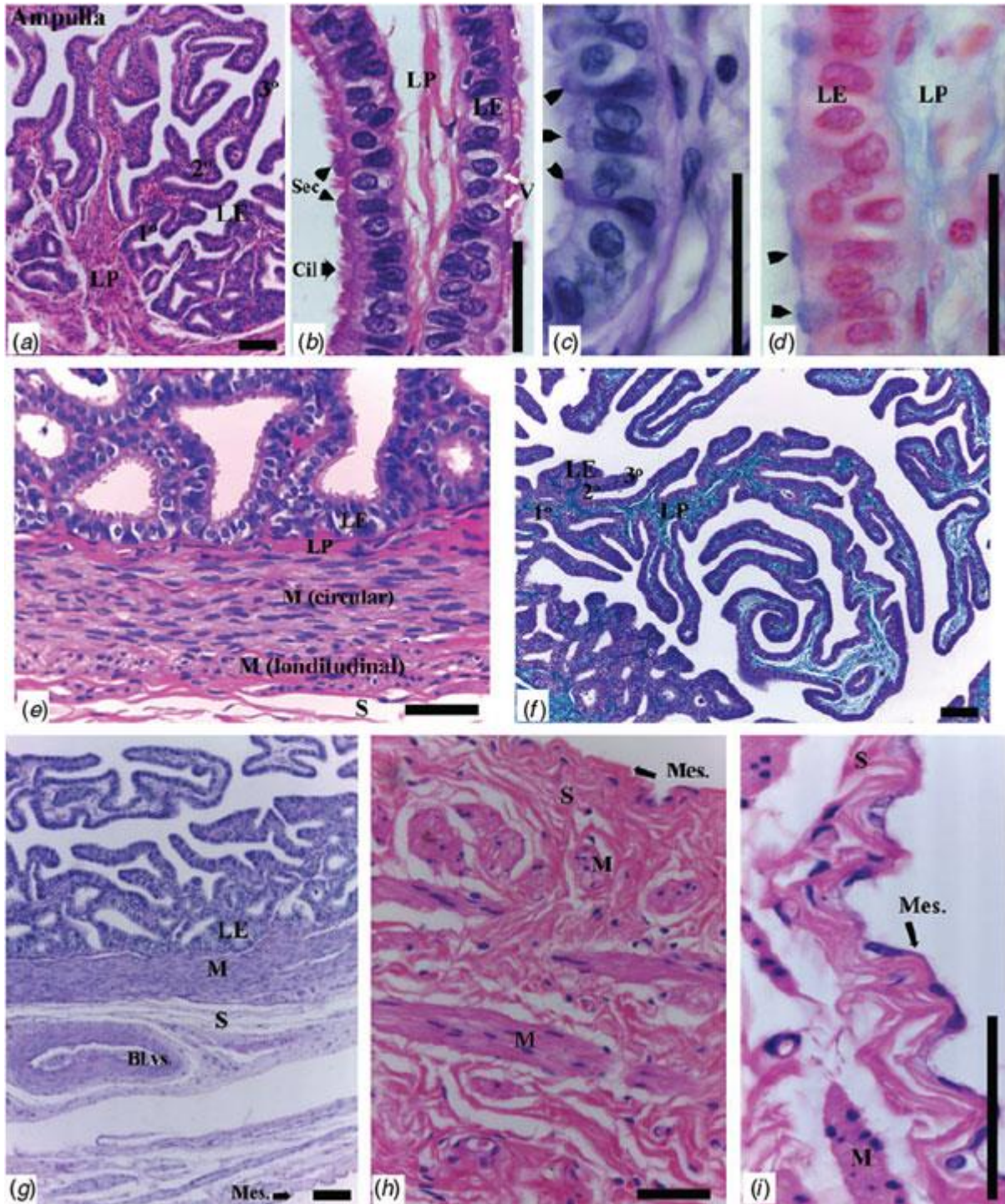
432 Underhill, C. (1992). CD44: the hyaluronan receptor. *J. Cell Sci.* 103, 293–298.

433 Wang, Q., and Margolis, B. (2007). Apical junctional complexes and cell polarity. *Kidney Int.* 72, 1448–
434 1458.

435 Weigel, P. H., Hascall, V. C., and Tammi, M. (1997). Hyaluronan synthases. *J. Biol. Chem.* 272, 13 997–
436 14 000.

- 437 Whittingham, D. G. (1968). Development of zygotes in cultured mouse oviducts. I. The effect of varying
438 oviductal conditions. *J. Exp. Zool.* 169, 391–397.
- 439 Xu, H., Ito, T., Tawada, A., Maeda, H., Yamanokuchi, H., Isahara, K., Yoshida, K., Uchiyama, Y., and Asari,
440 A. (2002). Effect of hyaluronan oligosaccharides on the expression of heat shock protein 72. *J. Biol.*
441 *Chem.* 277, 17 308–17 314.
- 442

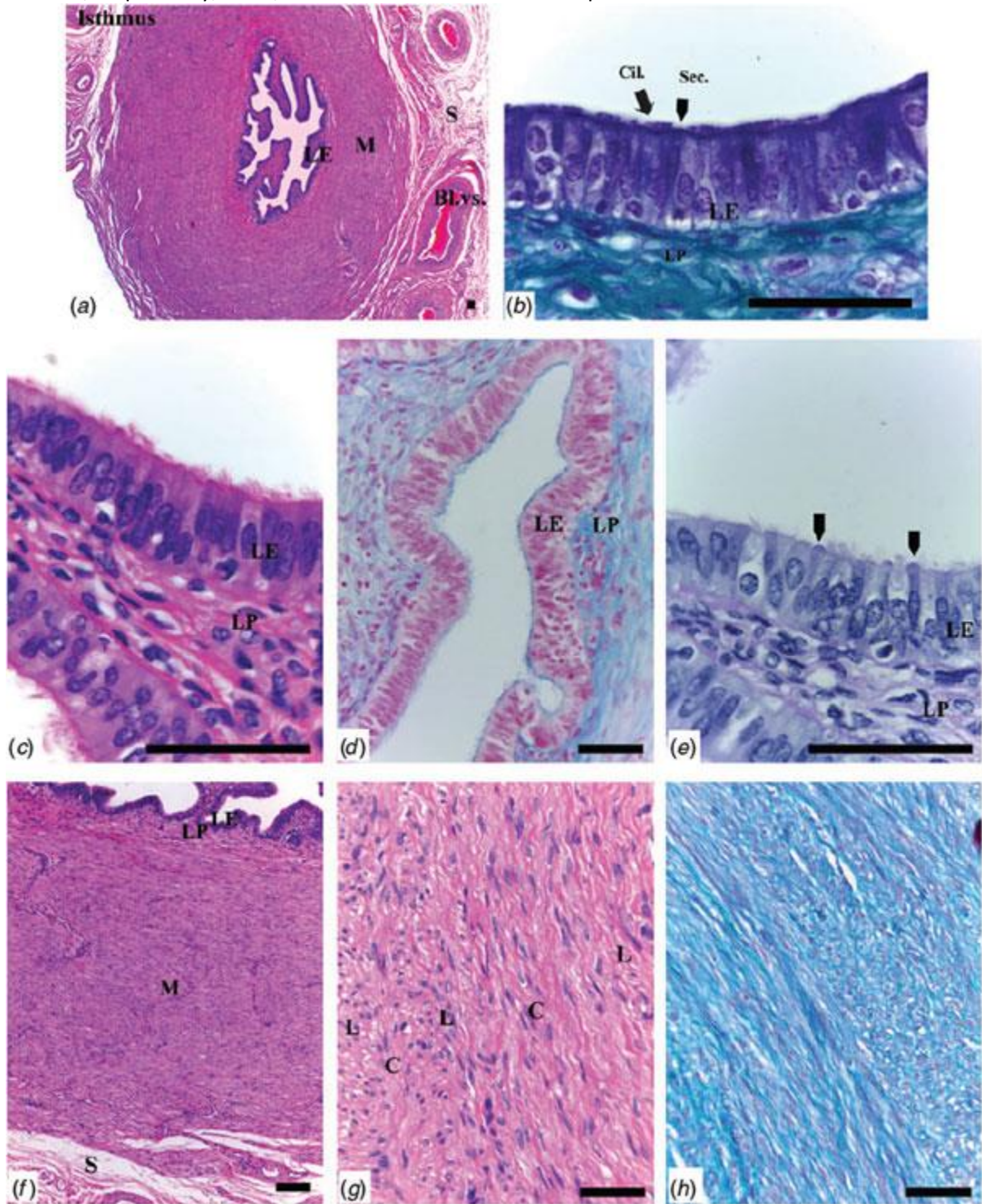
443 Fig. 1. Representative images showing the histological structure of the ampulla of the camel oviduct
 444 stained by (a, b, e, h, i) haematoxylin and eosin, (c, g) periodic acid-Schiff (PAS), (f) Crossman trichrome
 445 and (d) Alcian blue. The ampulla consisted of the lamina epithelialis (LE), lamina propria submucosa
 446 (LP), lamina muscularis (M) and outermost serosa (S). The LE and the underlining LP were highly folded
 447 into primary folds (1°), branching into secondary (2°) and tertiary (3°) folds. The LE consisted of
 448 secretory cells (Sec; black arrowheads) and non-secretory epithelial cells (Cil; black arrows). Some
 449 epithelial cells were vacuolated (V). Secretory cells (Sec) were positive for PAS (dark purple colour)
 450 and Alcian blue (blue colour). The serosa (S) was covered by mesothelium (Mes). Scale bars = 200 μ m.



451

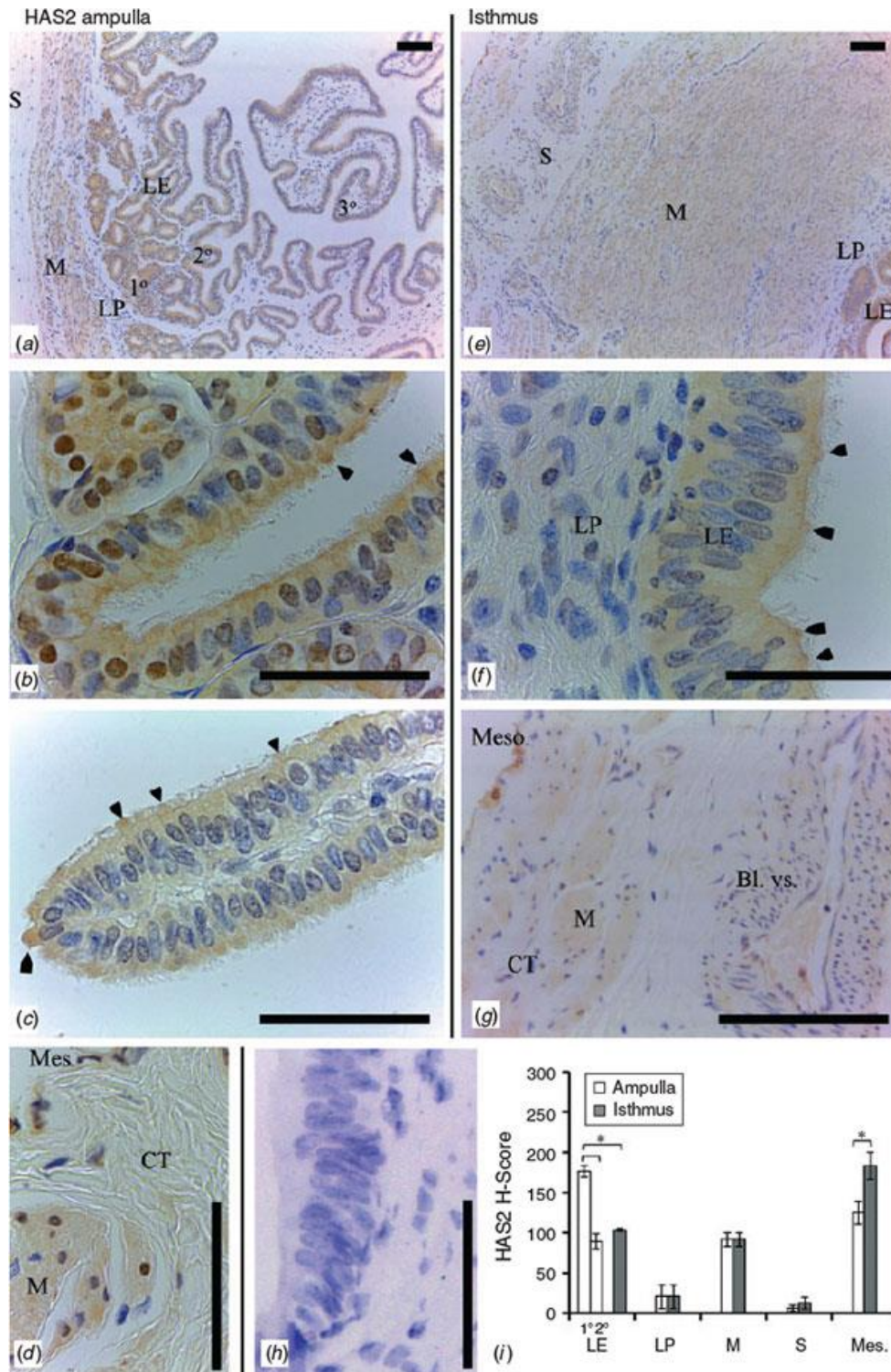
452

453 Fig. 2. Representative images showing histological structure of the isthmus of camel oviduct stained by (a, c, f, g) haematoxylin and eosin, (e) periodic acid-Schiff (PAS), (b, h) Crossman trichrome and ((d) 454 455 456 457 Alcian blue. LE, lamina epithelialis; LP, lamina propria submucosa; M, lamina muscularis; S, outermost serosa; arrowheads, secretory cells (Sec); Cil, ciliated cells; L, C, layers of longitudinal and circular muscles, respectively; Bl.vs., blood vessels. Scale bars = 200 μ m.



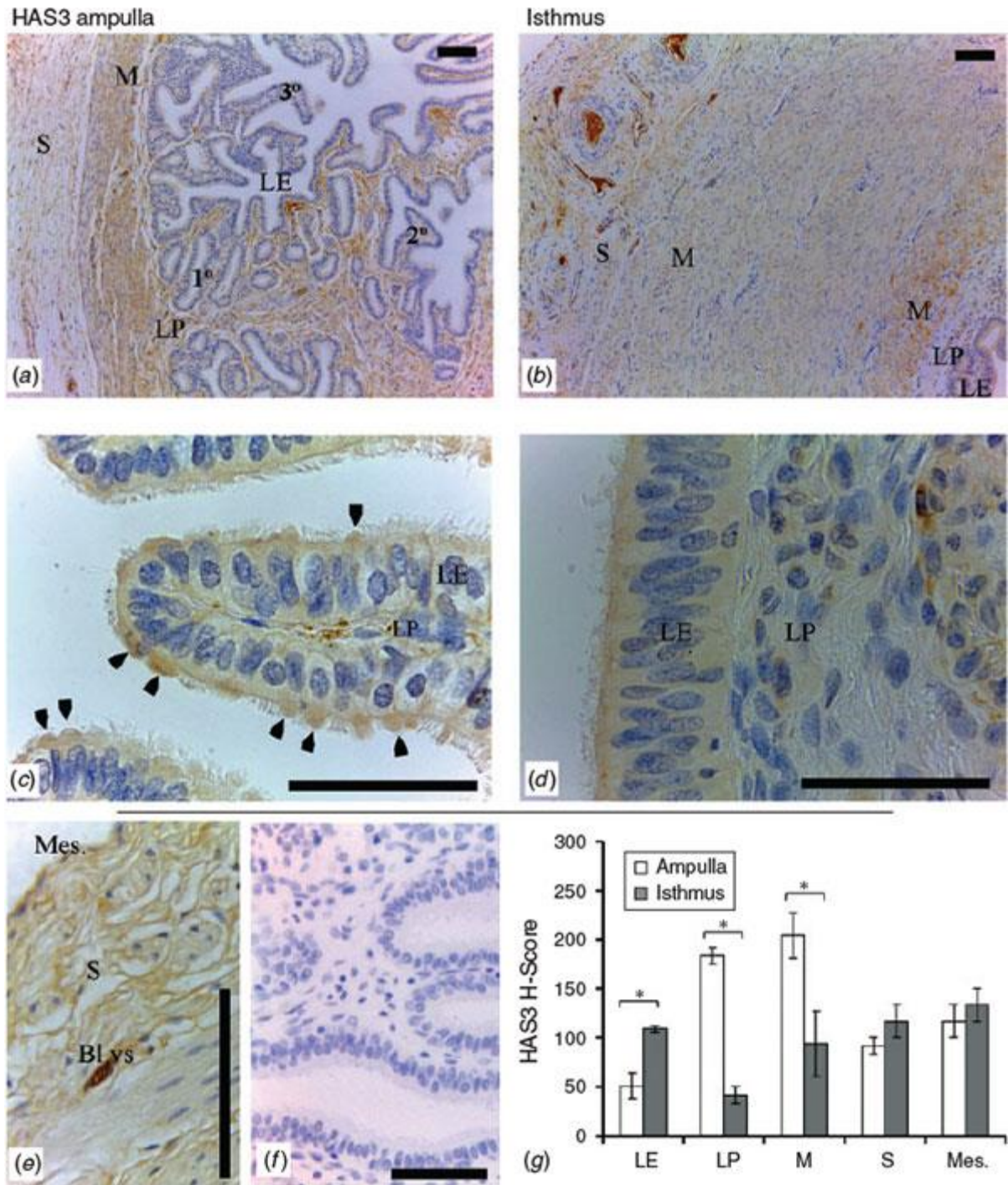
458

459 Fig. 3. Immunolocalisation of hyaluronic acid synthase (HAS) 2 in the (a–d) ampulla and (e–g)
 460 isthmus of the camel oviduct. HAS2 is shown as brown staining (diaminobenzidine), whereas nuclei
 461 are counterstained with haematoxylin (blue). (h) Negative control using normal rabbit IgG. LE,
 462 lamina epithelialis; LP, lamina propria submucosa; M, lamina muscularis; S, outermost serosa
 463 containing connective tissue (CT) and muscle bundles (M) and covered by mesothelium (Mes). 1°, 2°,
 464 3°, primary, secondary and tertiary folds of the mucosa in the ampulla, respectively; arrowheads,
 465 secretory cells (Sec). Scale bars = 200 μ m. (i) HSCORE for HAS2 immunostaining in different layers of
 466 the ampulla and isthmus. Data are the mean \pm s.e.m. *P < 0.05.



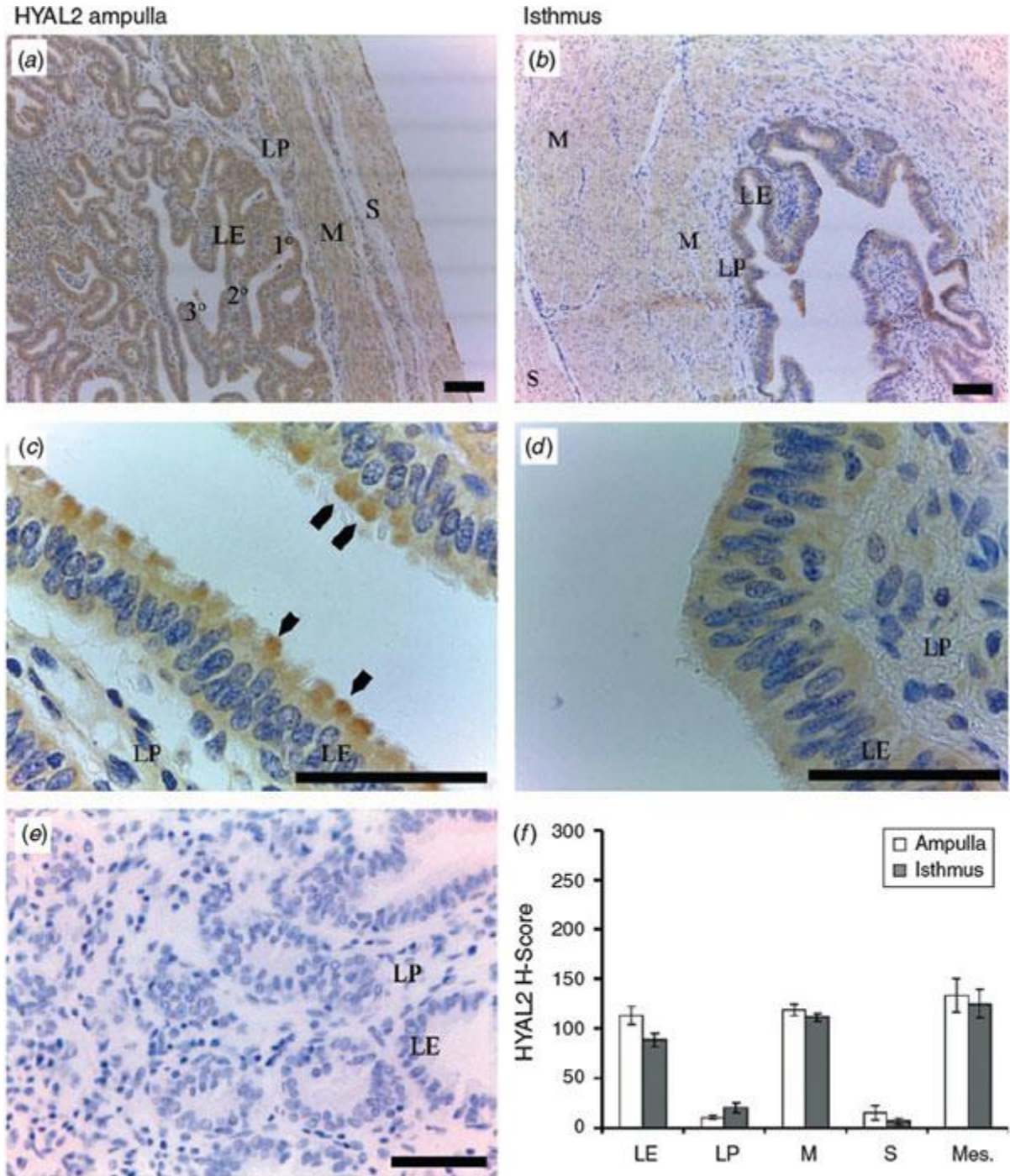
467

468 Fig. 4. Immunolocalisation of hyaluronic acid synthase (HAS) 3 in the (a, c) ampulla and (b, d, e)
 469 isthmus of the camel oviduct. (f) Negative control using normal rabbit IgG. HAS3 is shown as brown
 470 staining (diaminobenzidine), whereas nuclei are counterstained with haematoxylin (blue). LE, lamina
 471 epithelialis; LP, lamina propria submucosa; M, lamina muscularis; S, outermost serosa containing
 472 blood vessels (Bl.vs.) and covered by mesothelium (Mes); 1°, 2°, 3°, primary, secondary and tertiary
 473 folds of the mucosa in the ampulla, respectively; arrowheads, secretory cells (Sec). Scale bars = 200
 474 μm . (g) HSCORE for HAS3 immunostaining in different layers of the ampulla and isthmus. Data are
 475 the mean \pm s.e.m. * $P < 0.05$.



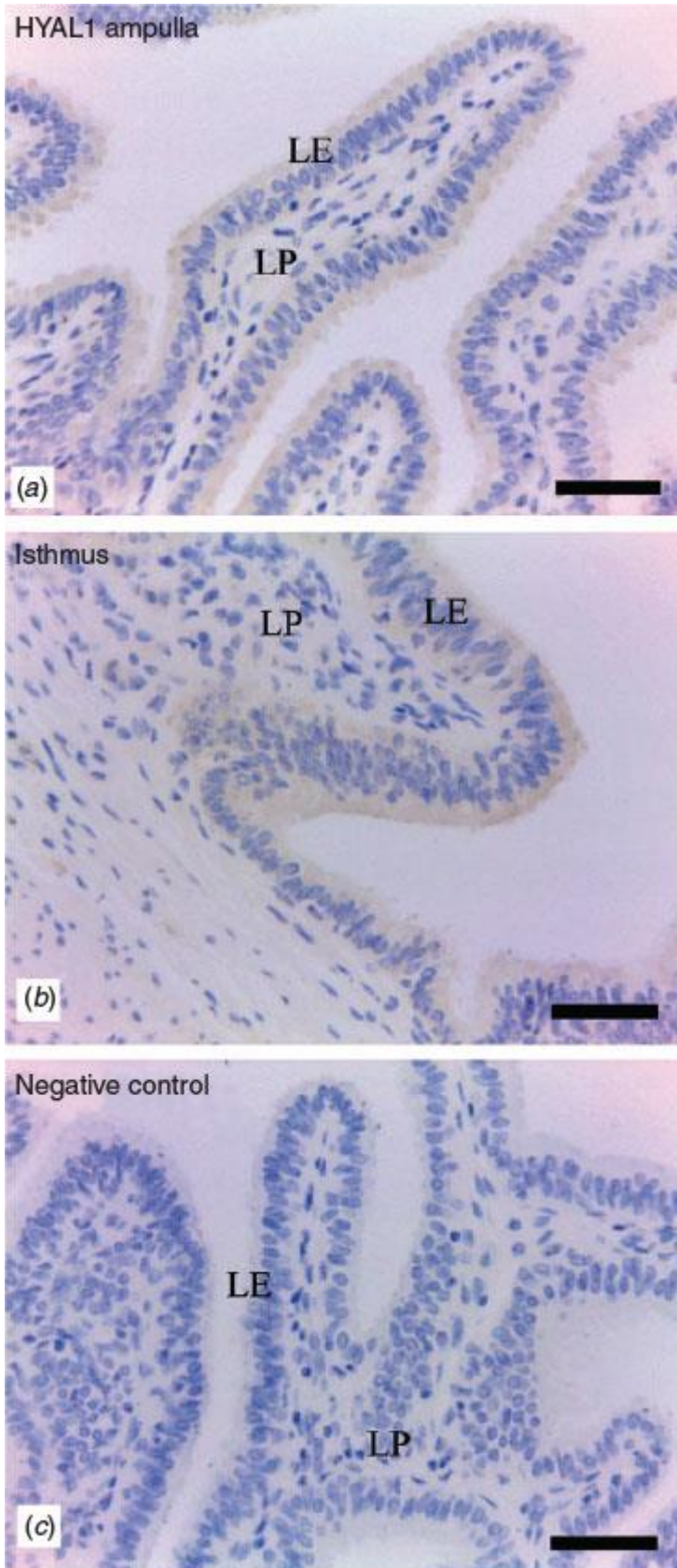
476
 477
 478

479 Fig. 5. Immunolocalisation of hyaluronidase (HYAL) 2 in the (a, c) ampulla and (b, d) isthmus of the
 480 camel oviduct. HYAL2 is shown as brown staining (diaminobenzidine), whereas nuclei are
 481 counterstained with haematoxylin (blue). (e) Negative control using normal rabbit IgG. LE, lamina
 482 epithelialis; LP, lamina propria submucosa; M, lamina muscularis; S, outermost serosa; 1°, 2°, 3°,
 483 primary, secondary and tertiary folds of the mucosa in the ampulla, respectively; arrowheads,
 484 secretory cells (Sec). Scale bars = 200 µm. (f) HSCORE for HYAL2 immunostaining in different layers
 485 of the ampulla and isthmus. Data are the mean ± s.e.m. No significant differences were detected at P
 486 < 0.05.



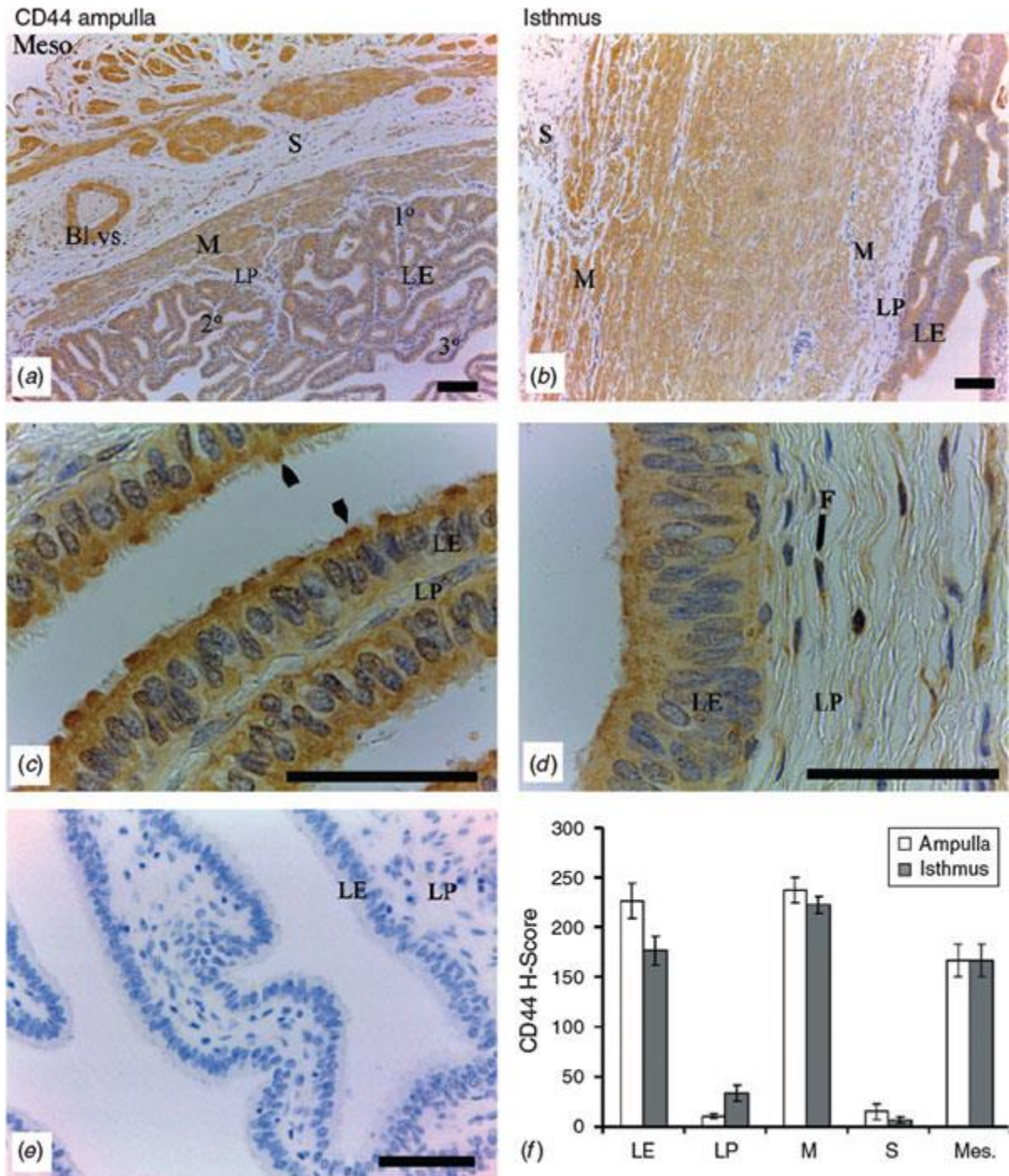
487
 488
 489

490 Fig. 6. Immunolocalisation of hyaluronidase (HYAL) 1 in the (a) ampulla and (b) isthmus of the camel
491 oviduct. HYAL1 is shown as brown staining (diaminobenzidine) while nuclei are counterstained with
492 haematoxylin (blue). (c) Negative control using normal rabbit IgG. LE, lamina epithelialis; LP, lamina
493 propria submucosa; M, lamina muscularis. Scale bars = 200 µm.



494

495 Fig. 7. Immunolocalisation of CD44v6 in the (a, c) ampulla and (b, d) isthmus of the camel oviduct.
 496 CD44v6 is shown as brown staining (diaminobenzidine), whereas nuclei are counterstained with
 497 haematoxylin (blue). (e) Negative control using normal mouse IgG. LE, lamina epithelialis; LP, lamina
 498 propria submucosa; M, lamina muscularis; S, outermost serosa; 1°, 2°, 3°, primary, secondary and
 499 tertiary folds of the mucosa in the ampulla, respectively; arrowheads, secretory cells (Sec); F,
 500 fibrocytes. Scale bars = 200 µm. (f) HSCORE for CD44v6 immunostaining in different layers of the
 501 ampulla and isthmus. Data are the mean ± s.e.m. No significant differences were detected at P <
 502 0.05.



503